Zeitschrift: Helvetica Physica Acta
Band: 55 (1982)
Heft: 6

Artikel: Low temperature structural and magnetic properties of PrPb_3
Autor: Niksch, M. / Assmus, W. / Lüthi, B.
DOI: https://doi.org/10.5169/seals-115305

Helvetica Physica Acta, Vol. 55 (1982) 688–698 0018–0238/82/060688–11$1.50 + 0.20/0

Low temperature structural and magnetic properties of $PrPb_3$

By M. Niksch,[1]) W. Assmus,[1]) B. Lüthi,[1]) Physikalisches Institut der Universität, 6000 Frankfurt a.M., FRG
H. R. Ott,[2]) Laboratorium für Festkörperphysik, ETH Hönggerberg, CH-8093 Zürich, Switzerland
J. K. Kjems, Risø National Laboratory, 4000 Roskilde, Denmark

(23. XI. 1982)

Abstract. Measurements of elastic constants and thermal expansion on a single-crystal specimen identify the low-temperature phase transition of $PrPb_3$ at 0.37 K as a Jahn–Teller type structural transition. Additional neutron-scattering experiments on the same sample confirm the nonmagnetic character of the transition. Large precursor effects in the thermal expansion indicate that structural deformations probably develop at temperatures well above the cooperative transition temperature, a phenomenon which may be a rather general feature of structural phase transitions.

I. Introduction

In a previous investigation of the low-temperature properties of polycrystalline $PrPb_3$, Bucher and collaborators found a temperature independent magnetic susceptibility below 5 K and a pronounced specific-heat anomaly below 1 K [1]. From this behaviour they identified the crystal-field ground state of the Pr^{3+} ($J = 4$) ions as a nonmagnetic Γ_3 doublet state. They did not, however, discuss the origin of the specific heat peak at 0.35 K. Subsequent inelastic neutron-scattering experiments could identify two crystal-field transitions out of the ground state, namely $\Gamma_3 - \Gamma_4(19.4\,\mathrm{K})$ and $\Gamma_3 - \Gamma_5(28.9\,\mathrm{K})$ [2].

With a nonmagnetic but Jahn–Teller active Γ_3 ground state, it is likely that the specific-heat anomaly is due to a cooperative structural transition. In this paper we give new experimental evidence supporting this conjecture. We present results from measurements of elastic constants, thermal expansion and neutron scattering on a single-crystalline sample of $PrPb_3$. We give a quantitative description of the temperature dependence of various thermodynamic functions, of magnetic excitations and of the mechanism driving the structural phase transition.

In the next section we briefly describe the growth of $PrPb_3$ single crystals and the various techniques which were used in the low-temperature measurements. We then show and interpret our various experimental results and finally we

[1]) Work supported by the Sonderforschungsbereich 65, Deutsche Forschungsgemeinschaft.
[2]) Work supported by the Schweizerischer Nationalfonds zur Förderung der wissenschaftlichen Forschung.

discuss some general aspects of structural phase transitions, driven by quadrupolar or Jahn–Teller type interactions.

II. Sample and experiments

Single crystals of $PrPb_3$ were grown from a tantalum crucible using the Czochralski technique. The material has a congruent melting point of 1120°C but has a high lead evaporation loss (v.p. > 10 mbar) at this temperature. The evaporation loss is kept to a minimum by growth under an argon atmosphere at a pressure of 20 bar. The tantalum crucible is enclosed in a quartz tube which is built into the growth chamber of an Arthur D. Little crystal-growth machine. The quartz tube prevents the lead vapor from contaminating the growth chamber and being deposited on the water cooled R.F. coil. Using a growth speed of 10 mm/hr, crystals of 15 mm diameter and 30 mm length have been grown.

Since the phase transition and hence the most interesting temperature range lies below 1 K, dilution refrigerator systems were used in all our experiments. For elastic constant measurements the ultrasonic sample holder was inserted into a refrigerator system with direct outside access to the mixing chamber [3]. The thermal expansion was measured with a specially designed capacitance dilatometer providing good thermal contact to the specimen. The neutron-scattering experiments were performed at the TAS-7 cold source triple-axis spectrometer at Risø in the temperature range from 0.09 to 4.2 K. The Bragg profiles showed that the sample consisted of several grains with an overall mosaic width of 0.9°, FWHM.

For further characterization the elastic constants were also measured up to 230 K.

III. Results and discussion

(a) *Elastic constants*

In Fig. 1 we show the experimentally determined elastic constants c_{44}, $c_{11}-c_{12}$ and $c_L=\frac{1}{2}(c_{11}+c_{12}+2c_{44})$ in the temperature region from 0.1 to 200 K. All three modes exhibit strong anomalous temperature dependences for $T<$ 100 K. The $c_{11}-c_{12}$ mode shows an overall softening of 15%. This is due to crystal field effects as observed before for many intermetallic rare-earth compounds [4].

First we discuss the temperature dependence of the symmetry elastic constants c_{44} and $(c_{11}-c_{12})/2$ in the region above the phase transition temperature $T>T_a=0.37$ K. In contrast to previous experiments we find, that in the case of $PrPb_3$ not only strong magnetoelastic coupling between strains and the quadrupole moments ($l=2$) of the Pr^{3+} ions but also higher order ($l=4$) moments have to be taken into account. Hence the magnetoelastic coupling reads [5]

$$\mathcal{H}_{me}=-\sum_i\{\varepsilon_2(g_3^{(2)}O_{2_i}^2\sqrt{3}+g_3^{(4)}O_{4_i}^2)+\varepsilon_3(g_3^{(2)}O_{2_i}^0+g_3^{(4)}O_{4_i}^0)+\varepsilon_{xy}(g_5^{(2)}O_{xy}+g_5^{(4)}\tilde{O}_4^2)\} \quad (1)$$

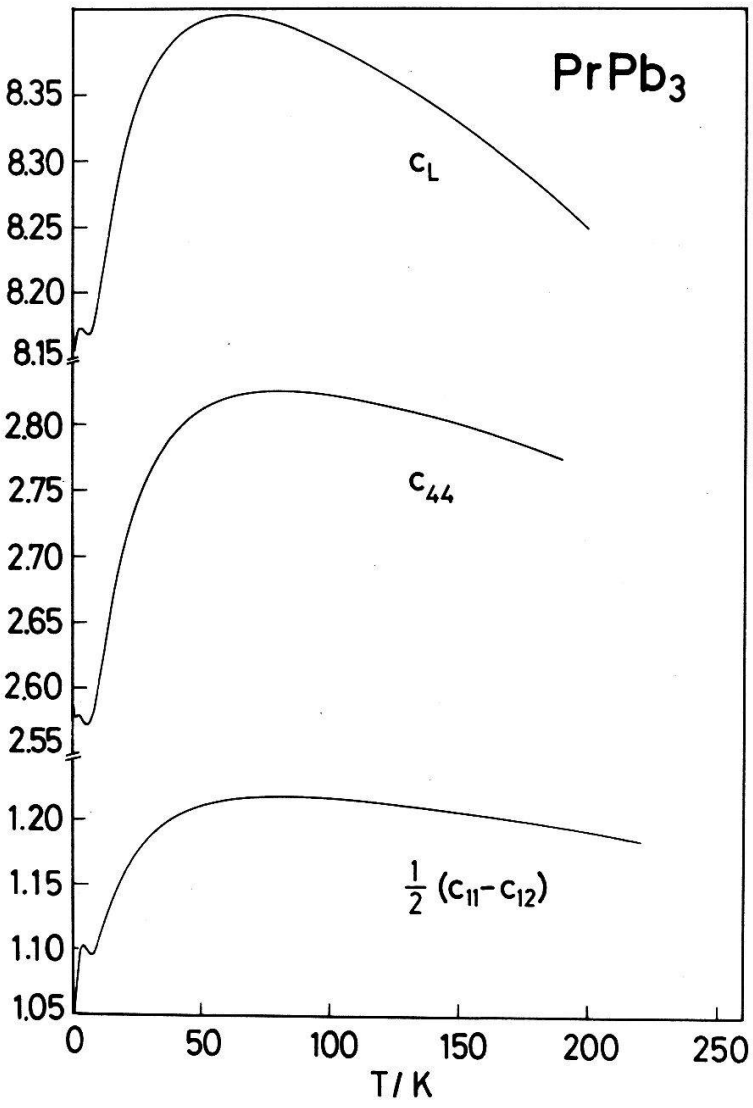

Figure 1
Temperature dependence of symmetry elastic constants $\frac{1}{2}(c_{11}-c_{12})$, c_{44} and $c_L=\frac{1}{2}(c_{11}+c_{12}+2c_{44})$ of a single crystal of $PrPb_3$ between 0.1 and 220 K.

where

$$\varepsilon_2=\frac{1}{\sqrt{2}}(\varepsilon_{xx}-\varepsilon_{yy}), \qquad \varepsilon_3=\frac{1}{\sqrt{6}}(2\varepsilon_{zz}-\varepsilon_{xx}-\varepsilon_{yy})$$

are the orthorhombic and tetragonal symmetry strains, $O_2^2=J_x^2-J_y^2$, $O_2^0=3J_z^2-J(J+1)$, $O_{xy}=J_xJ_y+J_yJ_x$ are the quadrupolar operators and as examples for $l=4$ operators we give

$$O_4^2=\tfrac{1}{4}[(7J_z^2-J(J+1)-5)(J_+^2+J_-^2)+(J_+^2+J_-^2)(7J_z^2-J(J+1)-5)]$$

$$\tilde{O}_4^2=\frac{-i}{4}[(7J_z^2-J(J+1)-5)(J_+^2-J_-^2)+(J_+^2-J_-^2)(7J_z^2-J(J+1)-5)]$$

For the elastic constants one obtains in the usual manner [4]:

$$c=c_\Gamma^0-g_\Gamma^2N\frac{\chi_{s\Gamma}}{1-K_\Gamma\chi_{s\Gamma}} \tag{2}$$

with c_Γ^0 denoting the background elastic constants, $\chi_{s\Gamma}$ the strain susceptibility $d\langle O_\Gamma\rangle/d\varepsilon_\Gamma$ and K_Γ a coupling constant describing quadrupolar interactions.

In Fig. 2 we present a fit of such a calculation to the experiment for the c_{44} and $c_{11}-c_{12}$ mode. For the c_{44}-mode we get a good fit with only quadrupolar magnetoelastic interaction. The calculation reproduces the experimentally observed minimum for $T\sim 6$ K and the subsequent flattening at low temperatures very nicely. On the other hand a pure quadrupolar coupling does not explain the temperature dependence of the $c_{11}-c_{12}$ mode (dotted line). It gives a continuous softening of the elastic mode due to the Γ_3 ground state, whereas experimentally a shallow minimum is observed for $T\sim 8$ K and a strong minimum close to the transition temperature T_a. Inclusion of $l=4$ terms with a coupling ratio $\delta = g_3^{(4)}/g_3^{(2)} = 1/135$ reproduces the salient features of the experimental behaviour although the fit is not perfect. However, there seem to be no other strain

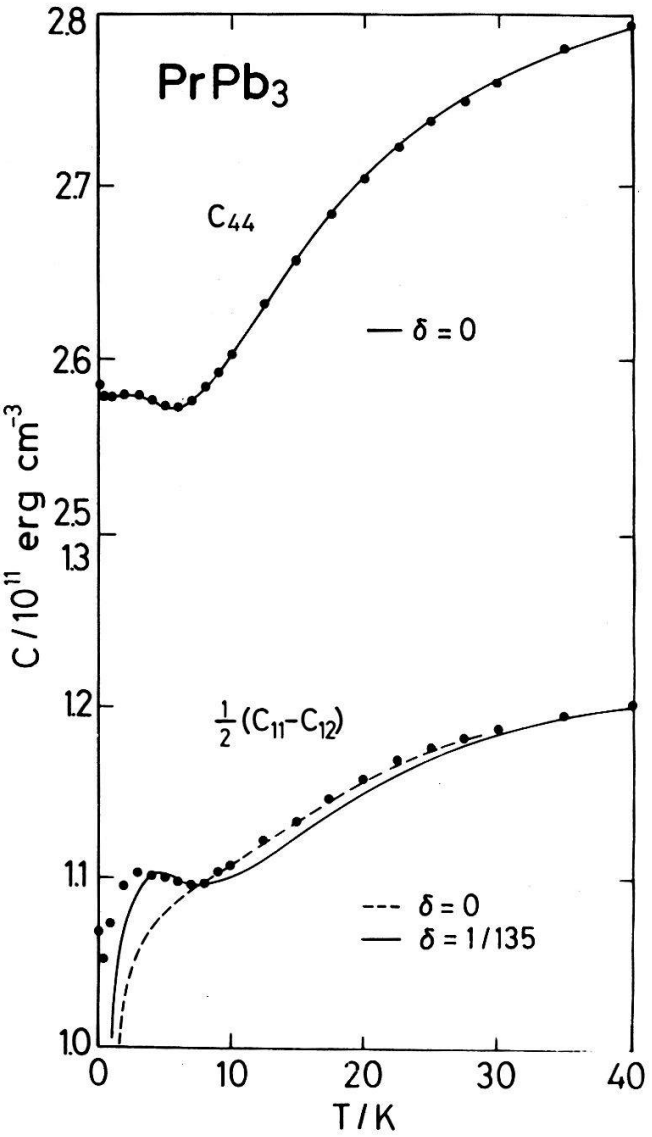

Figure 2
Temperature dependence of the elastic constants $\frac{1}{2}(c_{11}-c_{12})$ and c_{44} between 0.1 and 40 K. The lines are fits based on the CEF energy-level scheme given in Table 1.
c_{44}: solid line considers $l=2$ terms only.
$(c_{11}-c_{12})$: broken line considers $l=2$ terms only,
solid line includes terms with $l=2$ and $l=4$ (for explanations see text).

dependent interactions which could produce such an effect in the cubic, paramagnetic region.

We also mention that with the analogous $l=4$ interaction for the c_{44}-mode we can explain the temperature dependence of $c_{44}(T)$ for PrSb, a long standing problem. In this case one found experimentally [6] a minimum in c_{44} at $T=25$ K whereas a ($l=2$)-calculation gave a minimum at 60 K. Inclusion of $\tilde{O}_4^2$ operators gave a satisfactory fit [6] with $\delta = g_5^{(4)}/g_5^{(2)} = 1/45$. One obtains generally $\delta \sim 10^{-2}$ if one assumes that $g_\Gamma^{(4)}/g_\Gamma^{(2)}$ roughly follows an a^3/a^5 dependence (where a is the lattice constant).

A full fit to equation (2) gives the coupling constants g_3, g_5 and K listed in Table 1. From these coupling constants we can already deduce that the phase transition at T_a should be of cooperative Jahn–Teller type. This will be discussed in more detail below.

We now focus our attention to the vicinity of the phase transition. In Fig. 3 we show the temperature dependence of the elastic modes in the low-temperature region $T<4$ K. For the $(c_{11}-c_{12})/2$ mode one finds a pronounced minimum at 0.45 K, the softening amounting to 2% from 4 K for the sound velocity. The slope of the subsequent sharp rise decreases at 0.37 K. The c_{44}-mode is rather flat below 4 K and rises for $T<0.5$ K by about 0.1%. The c_L-mode exhibits a rather shallow minimum at $T\sim 0.5$ K. All these data indicate that a phase transition occurs for $T<0.5$ K. The elastic-constant data alone would point to a phase transition at $T=0.45$ K instead of the 0.37 K as indicated by thermal-expansion and specific-heat experiments discussed below. Further comments on this behaviour will be given in Section III(e).

(b) *Thermal expansion*

Figure 4 shows the temperature dependence of the linear-thermal-expansion coefficient α along the [110]-direction of the $PrPb_3$ single crystal below 1.3 K. It may be seen that a pronounced anomaly peaking at 0.37 K and thus determining the transition temperature T_a rests on another, much broader anomaly with a maximum at roughly 0.5 K and extending up to temperatures far above T_a. Additional measurements at higher temperatures indicate that the anomalous negative slope of $\alpha(T)$ is observed up to 4 K [7]. The temperature dependence of

Table 1
Physical parameters used in the calculations and/or deduced from our experiments.

Crystal-field splittings: $\Gamma_3-\Gamma_4(18.7\text{ K})-\Gamma_5(28.8\text{ K})$	
Structural transition temperature $T_a = 0.37$ K	
Density $\rho = 11.0\ \text{g cm}^{-3}$	
Elastic constants ($T=200$ K) (in 10^{11} erg cm^{-3})	$c_{44}=2.77,\quad \frac{c_{11}-c_{12}}{2}=1.19$
	$c_B=\frac{1}{3}(c_{11}+2c_{12})=5.09$
Debye temperature $\theta_D^{el}(T=0\text{ K})=135$ K	
Magnetoelastic coupling constants	$g_3^{(2)}=26.4$ K, $\quad g_3^{(4)}=0.2$ K
	$g_5^{(2)}=65.6$ K, $\quad g_5^{(4)}=0$
	$K\sim 0$
Elastic anisotropy factor	$A=\frac{2c_{44}}{c_{11}-c_{12}}=2.32\ (T=200\text{ K})$
	$=2.40\ (T=1\text{ K})$

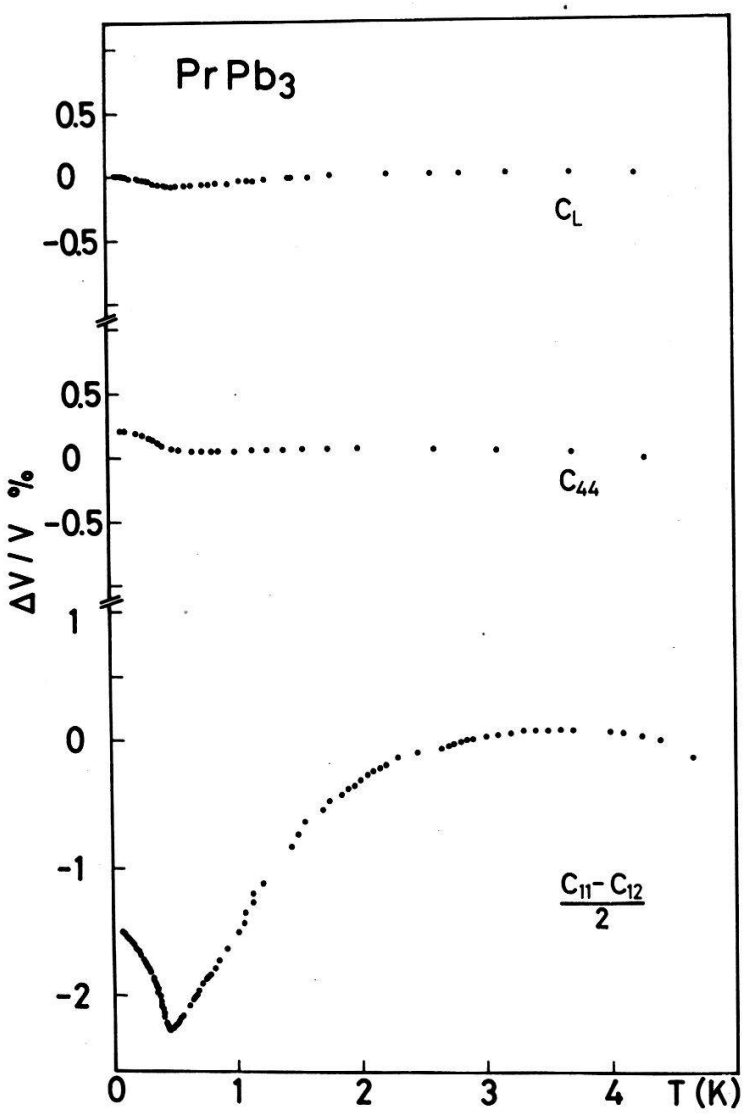

Figure 3
Temperature dependence of the elastic modes $\frac{1}{2}(c_{11}-c_{12})$, c_{44} and c_L, in the vicinity of the phase transition.

α as shown in Fig. 4 is very similar to that of the specific heat as reported in Ref. 1. We also note that this specific heat maximum occurs only 0.02 K below our thermal expansion coefficient maximum. Thermal expansion measurements on polycrystalline samples gave a similar broad anomaly without, however, the sharp peak at 0.37 K.

(c) *Neutron scattering*

The [200] and [011] Bragg peaks were carefully monitored in the temperature range from 4.2 to 0.09 K, especially around 0.4 K where the bulk measurements show evidence for a structural transition. No change was detected, which means that the macroscopic strains associated with the phase transition must be quite small with an upper limit of 0.1° for a possible change in the unit-cell angles.

With inelastic-neutron-scattering experiments we were able to determine the dispersion of the two crystal-field excitations ($\Gamma_3-\Gamma_4$, $\Gamma_3-\Gamma_5$) along the main symmetry directions. Examples of the constant-$\vec{q}$ inelastic scans are shown in Fig. 5, where one notices that both the energies and the relative intensity of the two

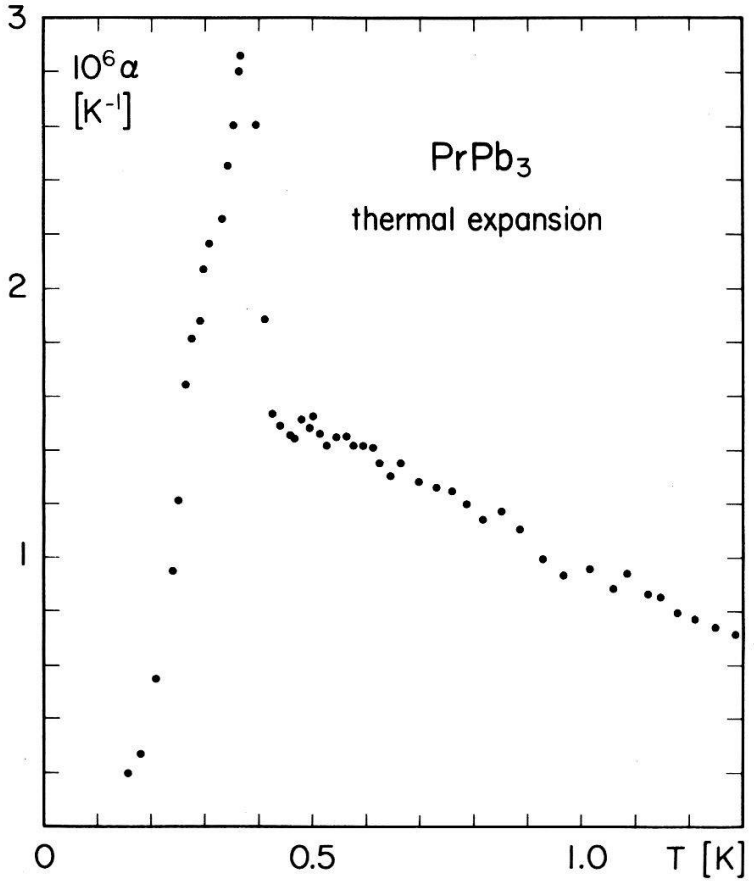

Figure 4
Linear-thermal-expansion coefficient along [110] of $PrPb_3$ between 0.15 and 1.3 K.

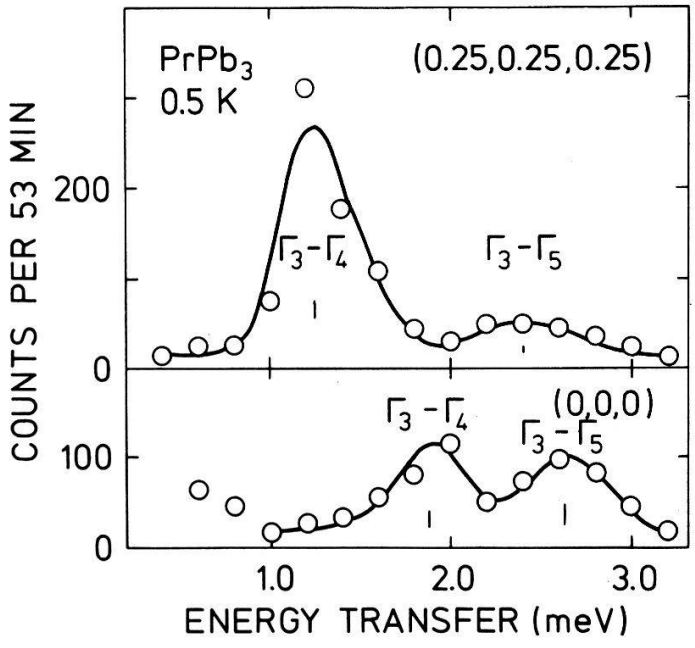

Figure 5
Inelastic neutron scattering spectra for two different values of the reduced momentum transfer $\vec{q} = (0, 0, 0)$ and $\vec{q} = (0.25, 0.25, 0.25)$.

transitions vary with the wavevector $\vec{q}$. The energy width remains constant at a value of 0.5 meV, much larger than the instrumental resolution of 0.2 meV. The lowest energy was found at $\vec{q}=(1/4, 1/4, 1/4)$ where $\hbar\omega_1 = 1.28$ meV and $\hbar\omega_2 = 2.40$ meV. This indicates a trend toward antiferromagnetic ordering with this wavevector but the exchange field is too small to overcome the crystal-field splitting. Hence $PrPb_3$ remains paramagnetic at least down to 0.09 K. In accordance with this, the inelastic spectra do not show any observable temperature dependence in the range $0.09 < T < 4.2$ K.

The spectra were analyzed with a simple RPA-model which takes into account only the J^z-transitions from the ground state to the two excited triplet states. The transition matrix elements are known to be $M_1^2 = |\langle\Gamma_3| J^z |\Gamma_4\rangle|^2 = 9.333$ and $M_2^2 = |\langle\Gamma_3| J^z |\Gamma_5\rangle|^2 = 4$. At temperatures below 4.2 K we can neglect the population of the excited states, and arrive at the following 2×2 dynamical matrix

$$\tilde{D} = \begin{Bmatrix} \omega_1^2 & -\omega_c^2 \\ -\omega_c^2 & \omega_2^2 \end{Bmatrix} \tag{3}$$

where

$$\omega_1^2 = \Delta_1(\Delta_1 - 2J(\vec{q})M_1^2) \qquad \omega_2^2 = \Delta_2(\Delta_2 - 2J(\vec{q})M_2^2)$$

$$\omega_c^2 = -2J(\vec{q})\sqrt{\Delta_1\Delta_2}M_2^* M_1$$

The eigenvalues correspond to the excitation energies Ω_1^2, and Ω_2^2 and the eigenvectors determine the intensities. This formalism leads to an excellent description of the observed spectra and the following iterative procedure was adapted in order to derive the best values for $J(\vec{q})$. First, both energies and intensities were fitted using the literature values for the crystal-field splittings Δ_1 and Δ_2 resulting in values for $\Omega_1(\vec{q})$, $\Omega_2(\vec{q})$ and $J(\vec{q})$ for each scan. Then these $J(\vec{q})$-results were used in simultaneous fits to all scans leading to new values for Δ_1 and Δ_2 and the procedure was repeated with a rapid convergence. The final results for the splittings are

$$\Delta_1(\Gamma_3 - \Gamma_4) = 1.61 \pm 0.05\text{meV}$$

and

$$\Delta_2(\Gamma_3 - \Gamma_5) = 2.48 \pm 0.05 \text{ meV}$$

The results for $\Omega_1(\vec{q})$, $\Omega_2(\vec{q})$, the normalized intensity ratio: $(I_1/I_2)\cdot(M_2^2/M_1^2)$, and $J(\vec{q})$ are shown in Fig. 6. The full curves are smooth lines through the best fit values and the dotted lines are the crystal-field-only results, i.e. $J(\vec{q}) \equiv 0$. One notices that the intensity variations are relatively more pronounced than the shifts in energy and it turned out in the analysis that the final values of $J(\vec{q})$ depend more sensitively on the observed intensities than on the observed energies with the actual experimental error. The shape of $J(\vec{q})$ corresponds to a dominating, negative next-nearest-neighbour exchange constant. However, this simple model would predict $J(1/4, 1/4, 1/4) = 0$, whereas a positive value is observed. Calculations of dispersion curves using only nearest-neighbour excitations [2] are therefore not adequate to describe our experimental results.

In summary, the inelastic-neutron-scattering spectra confirm the crystal-field level scheme for $PrPb_3$ and it rules out the possibility of magnetic ordering at

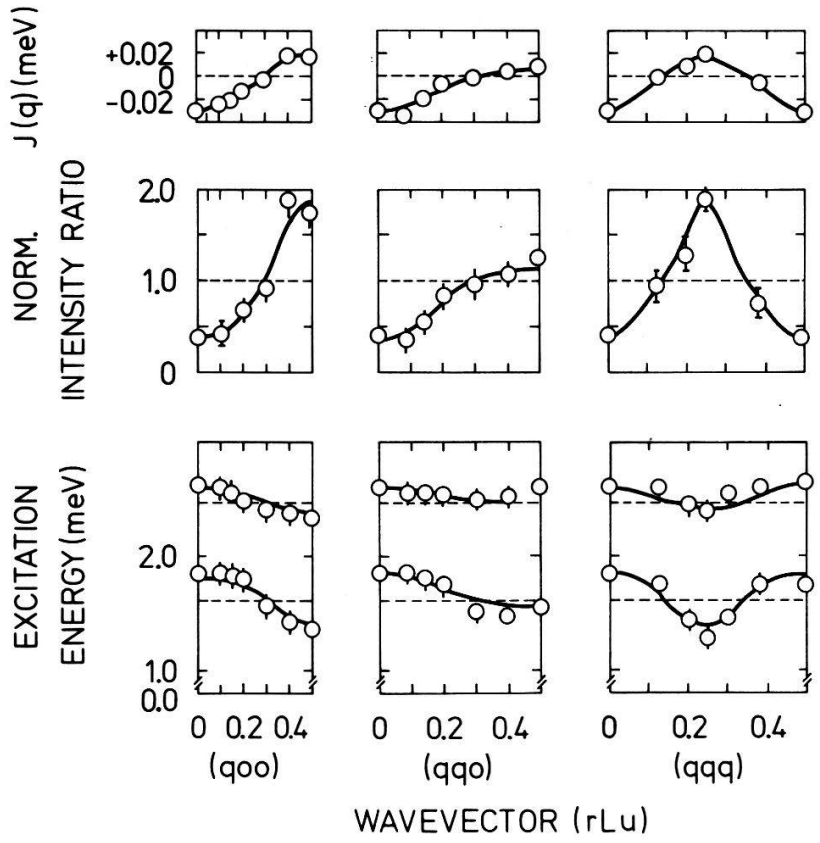

Figure 6
The variation with reduced momentum transfer along the main symmetry direction for the crystal-field excitation energies, the corresponding intensity ratios $(\Gamma_3-\Gamma_5)/(\Gamma_3-\Gamma_4)$, and the exchange energy $J(\vec{q})$ as determined by fits to the neutron-scattering spectra.

0.37 K. All the data are excellently reproduced by a simple RPA-model which assumes an isotropic exchange coupling acting on both the $\Gamma_3-\Gamma_4$ and $\Gamma_3-\Gamma_5$ transitions. The dominating exchange coupling is antiferromagnetic to the next nearest neighbour across the cube-face diagonal.

(d) *Phase transition aspects*

All the experimental evidence given in previous sections (elastic constants, thermal expansion, neutron scattering evidence) allow us to describe the phase transition to be of cooperative Jahn–Teller type [9] involving a tetragonal ε_3-strain. From the coupling constants deduced from the experiment we notice that the pure strain coupling amounts to more than 80% of the total coupling constant (see Table 1). We therefore only consider the magneto-elastic coupling and take $g^{(2)}_{\Gamma_3} = g = 30$ K in order to make some estimates.

Since the first excited crystal-field state (Γ_4) lies 19 K above the ground state Γ_3 level, we can neglect all the excited levels for the equilibrium aspects of the phase transition for $T < 0.5$ K. From the free energy density

$$F = \frac{c_\Gamma}{2}\varepsilon_\Gamma^2 - kTN \ln\left(\sum_i e^{-\beta E_i(\varepsilon_\Gamma)}\right) \tag{4}$$

we obtain an order-parameter equation for the spontaneous strain

$$\varepsilon_3 = \frac{N}{c_{11}-c_{12}} \frac{\sum_i \left(\frac{\partial E_i}{\partial \varepsilon_3}\right) e^{-\beta E_i}}{\sum_i e^{-\beta E_i}} \tag{5}$$

where E_i are the two Γ_3-levels, $E(\Gamma_3^1) = 8g\varepsilon_3$, $E(\Gamma_3^2) = -8g\varepsilon_3 - 12g^2\varepsilon_3^2$.

With these values we obtain a phase transition at $T_a = 0.37\,\mathrm{K}$ and an equilibrium strain at $T = 0$ of $\varepsilon_3 = 0.16\%$ or a volume conserving linear strain $\delta c/a = 0.13\%$. These estimates explain the failure of observing any structural changes with neutron-scattering techniques. With a mosaic spread of 0.9^0 it is impossible to observe splittings of 0.1^0. Furthermore the calculated $E(\Gamma_3)$-splitting at $T = 0\,\mathrm{K}$ amounts to $\Delta E = 16g \cdot \varepsilon_3 = 0.76\,\mathrm{K}$ again below the resolution of inelastic neutron techniques.

Within this simple model calculation one obtains a complete softening of the $c_{11} - c_{12}$ elastic constant when approaching T_a from higher temperatures and a mean-field type anomaly for the specific heat and thermal expansion below T_a. Clearly our experimental results are in disagreement with these predictions. The elastic constant $c_{11} - c_{12}$ only softens by about 15% and both the specific heat and the thermal expansion reveal anomalous contributions far above T_a.

At this point we should like to mention that similar features have been observed in thermal expansion data of other materials exhibiting structural phase transitions as e.g. UPd_3 [10] or V_3Si [11], and this seems to be a general feature of materials exhibiting martensitic transformations [12]. It is known that for materials with an elastic anisotropy parameter $A = 2c_{44}/(c_{11} - c_{12}) > 1$, a gradual growth of unstable dislocations is favoured [12]. For $PrPb_3$, A is about 2.4 (see Table 1). We therefore argue, that in our case, structural deformations develop already well above the cooperative transition temperature, giving rise to specific heat and thermal expansion contributions as observed. $R \ln 2$, the entropy associated with the splitting of the Γ_3 ground state is only reached in $PrPb_3$ when the specific heat reported in Ref. 1 is integrated to temperatures above 1 K. We therefore suggest that all these precursor effects in thermal expansion, specific heat and elastic constants are strongly influenced by gradual local structural changes.

(e) *Structural transitions in intermetallic compounds containing f-electrons*

While there are many examples of magnetic phase transitions in intermetallic rare-earth and actinide compounds, pure structural phase transitions are rare. In fact we only know of five: TmCd [13], TmZn [13], $PrCu_2$ [14, 15], $PrPb_3$ and UPd_3 [10]. if one describes the phase transitions with a structural molecular field Hamiltonian of the form

$$\mathcal{H} = -g_\Gamma \varepsilon_\Gamma O_\Gamma - K_\Gamma \langle O_\Gamma \rangle O_\Gamma \tag{6}$$

one can distinguish between the two limiting cases [16] where $g_\Gamma N/c_\Gamma \ll K_\Gamma$ and $g_\Gamma N/c_\Gamma \gg K_\Gamma$. The former case is usually denoted as quadrupolar transition, the latter as cooperative Jahn–Teller transition. Whereas TmCd and TmZn belong to the quadrupolar case, $PrPb_3$ is, according to our analysis, a typical representative

of a cooperative-strain type Jahn–Teller phase transition, $PrCu_2$ is an intermediate case with a dominating magnetoelastic interaction.

It is interesting to note that within the family of intermetallic rare-earth compounds, only compounds with Tm^{3+} and Pr^{3+} ions exhibit such electronic structural transitions. The reason for this lies in the rather large orbital moment L for these ions (Tm^{3+} ($J=6$, $L=5$), Pr^{3+} ($J=4$, $L=5$)). On the other hand there are many cases where structural and magnetic transitions coincide. These cases can be treated with models as the one given above, including a magnetic exchange term. Especially the case of Tb-pnictides has been treated in detail [17].

Acknowledgements

Helpful advice from Jens Jensen concerning the analysis of the neutron data is acknowledged.

REFERENCES

[1] E. Bucher, K. Andres, A. C. Gossard and J. P. Maita, Proc. Int. Conf. Low Temperature Physics, LT 13, Vol. 2, eds. K. D. Timmerhaus, W. J. O'Sullivan and E. F. Hammel, (Plenum Press, New York, 1974), p. 322.
[2] W. Gross, K. Knorr, A. P. Murani and K. H. J. Buschow, Z. Phys. *B37*, 123 (1980).
[3] G. Binnig and H. E. Hoenig, J. Physique Colloque *C6*, 1148 (1978).
[4] B. Lüthi, Dynamical Properties of Solids, Vol. 3, eds. G. K. Horton and A. A. Maradudin, (North Holland, Amsterdam 1980), p. 247.
[5] E. R. Callen and H. B. Callen, Phys. Rev. *129*, 578 (1963); E. du Tremolet de Lacheisserie, P. Morin and J. Rouchy, Ann. Physique *3*, 479 (1978).
[6] B. Lüthi, M. E. Mullen and E. Bucher, Phys. Rev. Letters *31*, 95 (1973).
[7] H. R. Ott and M. Gmür, unpublished results.
[8] B. Lüthi, M. Niksch, R. Takke and W. Assmus, IV Int. Conf. on Crystal Electric Field and Structural Effects in *f*-electron Materials, Wroclaw 1981 (Plenum Press), in print.
[9] G. A. Gehring and K. A. Gehring, Rep. Progr. Phys. *38*, 1 (1975).
[10] H. R. Ott, K. Andres and P. H. Schmidt, Physica *102*B, 148 (1980).
[11] B. S. Chandrasekhar, H. R. Ott and B. Seeber, Solid State Comm. *39*, 1265 (1981).
[12] N. Nakanishi, Progress in Materials Science *24*, 143 (1980) (Pergamon Press Ltd.).
[13] B. Lüthi, R. Sommer and P. Morin, J. Mag. Magn. Mat *13*, 198 (1979).
[14] K. Andres, P. S. Wang, Y. H. Wong, B. Lüthi and H. R. Ott, AIP Conf. Proc. *34*, 222 (1976).
[15] J. K. Kjems, H. R. Ott, S. M. Shapiro and K. Andres, J. Phys. Colloque *C6*, 1010 (1978).
[16] P. M. Levy, P. Morin, D. Schmitt, Phys. Rev. Letters *42*, 1417 (1979).
[17] J. Kötzler, G. Raffius, Z. Phys. *B38*, 139 (1980).